Nanomedicine: Nanotechnology, Biology, and Medicine 55 (2024) 102722

Contents lists available at ScienceDirect

Nanomedicine: Nanotechnology, Biology, and Medicine

journal homepage: www.sciencedirect.com/journal/nanomedicine-nanotechnology-biology-and-medicine

Defined covalent attachment of three cancer drugs to DNA origami increases cytotoxicity at nanomolar concentration

Natalia Navarro, MSc [a,b,1], Anna Aviñó, PhD [a,b], Òscar Domènech, PhD [c,d], Jordi H. Borrell, PhD [c,d], Ramon Eritja, PhD [a,b,*], Carme Fàbrega, PhD [a,b,1,*]

[a] Nucleic Acids Chemistry Group, Institute for Advanced Chemistry of Catalonia (IQAC-CSIC), Barcelona 08034, Spain
[b] Networking Center on Bioengineering, Biomaterials and Nanomedicine (CIBER-BBN), Barcelona 08034, Spain
[c] Physical Chemistry Section, Faculty of Pharmacy and Food Sciences, University of Barcelona (UB), Barcelona 08028, Spain
[d] Institute of Nanoscience and Nanotechnology (IN2UB), University of Barcelona (UB), Barcelona 08028, Spain

ARTICLE INFO

Keywords:
DNA nanotechnology
DNA origami
Covalent conjugation
Drug conjugates
cancer nanomedicine
Combination therapy

ABSTRACT

DNA nanostructures have captured great interest as drug delivery vehicles for cancer therapy. Despite rapid progress in the field, some hurdles, such as low cellular uptake, low tissue specificity or ambiguous drug loading, remain unsolved. Herein, well-known antitumor drugs (doxorubicin, auristatin, and floxuridine) were site-specifically incorporated into DNA nanostructures, demonstrating the potential advantages of covalently linking drug molecules via structural staples instead of incorporating the drugs by noncovalent binding interactions. The covalent strategy avoids critical issues such as an unknown number of drug-DNA binding events and premature drug release. Moreover, covalently modified origami offers the possibility of precisely incorporating several synergetic antitumor drugs into the DNA nanostructure at a predefined molar ratio and to control the exact spatial orientation of drugs into DNA origami. Additionally, DNA-based nanoscaffolds have been reported to have a low intracellular uptake. Thus, two cellular uptake enhancing mechanisms were studied: the introduction of folate units covalently linked to DNA origami and the transfection of DNA origami with Lipofectamine. Importantly, both methods increased the internalization of DNA origami into HTB38 and HCC2998 colorectal cancer cells and produced greater cytotoxic activity when the DNA origami incorporated antiproliferative drugs. The results here present a successful and conceptually distinct approach for the development of DNA-based nanostructures as drug delivery vehicles, which can be considered an important step towards the development of highly precise nanomedicines.

Introduction

The possibility of engineering artificial nanostructures using DNA molecules proposed by N. Seeman[1] with follow-up by P. Rothemund[2] opened up an attractive avenue with unlimited applications including imaging,[3,4] biosensing,[5,6] materials organization,[7,8] and drug delivery.[9,10] Recent decades have confirmed the tremendous potential of DNA nanotechnology, drawing increasing attention to the field due to its significant impact on the development of materials and nanoscience.[11]

Drug delivery is one of the most fascinating applications in which DNA nanostructures are used as carriers to deliver therapeutic molecules. Apart from increasing the solubility of drugs, the ease of synthesis of nucleic acids, high payload capacity, good biocompatibility and low cytotoxicity make DNA-based nanoscaffolds such as DNA origami attractive structural building blocks for biomedical applications.[12–14]

Moreover, due to their editable characteristics, staples can be chemically modified with a wide range of functional entities (e.g., aptamers,[15] lipids,[9] proteins,[16,17] and therapeutic oligonucleotides[18]) that can be site-specifically incorporated for different purposes. Importantly, one of the most significant applications involves developing novel cancer therapies.[19]

Despite extensive research on DNA nanostructures as drug delivery vehicles, chemotherapeutic drugs are still loaded into them using non-covalent binding modes, including intercalation,[20,21] groove binding[22] or simple electrostatic binding.[23] The vast majority of these studies have focused on the intercalation of doxorubicin between C-G base pairs and

* Corresponding authors at: Nucleic Acids Chemistry Group, Institute for Advanced Chemistry of Catalonia (IQAC-CSIC), Barcelona 08034, Spain.
E-mail addresses: ramon.eritja@iqac.csic.es (R. Eritja), carme.fabrega@iqac.csic.es (C. Fàbrega).
[1] These authors contributed equally to this work.

https://doi.org/10.1016/j.nano.2023.102722
Received in revised form 3 November 2023;
Available online 24 November 2023

binding to the minor groove in A-T rich regions of double-stranded DNA.[17,21,24–31] In addition to doxorubicin, other anthracyclines such as daunorubicin,[20] taxanes such as paclitaxel,[23] and cisplatin[32] have been incorporated in a similar way. Although these approaches are straightforward, there is no consensus about the methodology or conditions under which such studies should be performed, intercalation may lead to structural distortions or destabilization of the DNA nanostructures due to unwinding of the double helices,[33] and they do not provide the possibility of quantifying the drug loaded into the DNA nanostructure in a precise manner. Therefore, there is no precise spatial orientation or quantitative control of the loading of the agent into the nanocarrier or its release before reaching the site of action. The development of strategies to specifically incorporate antitumor molecules and take advantage of the possibility of controlling the spatial organization of the drugs are needed to improve the use of DNA origami as a nanocarrier. Moreover, approaches that offer the possibility of incorporating drug molecules other than those with the ability to intercalate DNA are also needed.

In terms of cellular internalization, folic acid-modified DNA nanostructures have been shown to be capable of binding to cancer cells overexpressing the folate receptor (FOLR1) and of delivering them in higher amounts than unmodified DNA-based nanostructures, suggesting that folic acid is a potential enhancer of drug uptake by tumor cells.[34–36]

In this study, we describe DNA origami inspired by the "magic bullet" concept coined by Paul Ehrlich.[37] Herein, we exploited the unique potential of DNA origami to control the spatial organization of several antitumor molecules and consequently to define the exact relative concentration in each DNA origami nanostructure, which may present a significant opportunity to enhance drug effectiveness and improve safety profiles. Our aim is to incorporate defined amounts of several drugs that act through different mechanisms in cancer chemotherapy, mirroring the approach commonly employed in combination therapies. To achieve this goal, we need to develop functionalization protocols that enable the incorporation of cancer drugs into DNA staples. By doing so, hybridization will generate "molecular pills" with precise and predefined compositions, which intercalation protocols cannot accomplish. Since this goal has never been reached, our study focuses on studying the functionalization of staples with several anticancer drugs and we aim to verify that the presence of modified staples does not impede the formation of DNA origami structures. We propose to use a rectangular DNA origami as an illustrative example of DNA nanostructures, which serve as biocompatible platforms for controlled incorporation of three different antitumor drugs, doxorubicin, floxuridine as a decanucleotide (FdU_{10}), and auristatin, to target the folate receptors that are overexpressed in cancer cells. To pursue this goal, the mentioned drugs and folic acid were site-specifically incorporated into DNA origami by chemical conjugation to structural staples. Different positions for each drug were selected to study synergic cytotoxicity effects. The evaluated drugs have different mechanisms of action in cells, which could lead to higher apoptotic activity in tumor cells and avoid the drawbacks of single compound treatment, such as drug resistance, side toxicity due to higher dosing or premature drug breakdown by metabolism. To our knowledge, this is the first time that three different drugs have been introduced in predefined positions of DNA origami, demonstrating that the incorporation of a relative short number of drug-modified staples can induce an important increase in cytotoxic effect of DNA nanostructures.

Materials and methods

Materials

M13mp18 single-stranded DNA (7249 nucleotides) was purchased from New England Biolabs (Massachusetts). Standard phosphoramidites, ancillary reagents and solvents for oligonucleotide synthesis were purchased from Applied Biosystems (USA). DNA purification cartridge from Glen Research. NAP-10 column (GE Healthcare (Little Chalfont, UK)). A plate of customized oligonucleotides was purchased from Sigma Genosys (St. Louis, MO, USA). Dead Cell Apoptosis Kit (FITC-Annexin V & Propidium Iodide), 1 Kb Plus DNA Ladder, Dulbecco's modified Eagle's medium (DMEM) and fetal bovine serum (FBS) were purchased from Thermo Fisher Scientific Inc. (Massachusetts). Doxorubicin, folic acid, methyl-β-cyclodextrin, and sucrose were purchased from Sigma (St. Louis, MO, USA). Auristatin maleimide was kindly provided by Dr. Mangues (Hospital de la Santa Creu i Sant Pau, Barcelona, Spain). Lipofectamine 2000 was purchased from Life Technologies (USA). Centrifugation devices, Nanosep 10 K omega were purchased to Pall Life Science (PALL, Puerto Rico). PE-FOLR1 antibody, DAPI, WGA-Alexa 555, and Cytochlasin D were purchased from Santa Cruz Biotechnology, Inc. (Dallas). All other common chemical reagents were purchased from Sigma-Aldrich (Missouri).

Methods

Synthesis of staples carrying FdU_{10} at the 3′ end

Oligonucleotide staples carrying FdU_{10} at the 3′ end were synthesized using controlled pore glass (CPG) functionalized with a 3′-succinyl-5′-dimethoxytrityl (DMT)-FdU solid support. FdU was protected with the dimethoxytrityl (DMT) group and then was treated with succinic anhydride to obtain the corresponding hemisuccinate as described.[38] Finally, the controlled pore glass solid support with 5-FdU was prepared following standard protocols.[39,40] FdU_{10}-modified staples were assembled with the corresponding commercially available DMT-protected FdU and DMT/isobutytryl, benzoyl-base-protected natural 2′-deoxynucleoside 2-cyanoethyl phosphoramidites in 1 μmol scale. After sequence assembly, the oligonucleotide-CPG supports were deblocked with concentrated ammonia overnight at 55 °C. Deprotection of the control FdU_{10} sequence was performed overnight at room temperature, followed by 1 h at 55 °C.

Synthesis of the doxorubicin oligonucleotide conjugates

First, doxorubicin was reacted with the *N*-hydroxysuccinimide ester. Then, the resulting maleimide derivative was reacted with a 5′-thiol-oligonucleotide. In brief, 0.45 mg (846 nmol) of doxorubicin were dissolved in 25 μl of DMSO. Then, 45 μl of an 18.5 mM solution of *N*-ε-malemidocaproyl-oxysuccinimide ester (EMCS) and 30 μl of DMSO were added to the doxorubicin solution. The reaction proceeded for 2 h with gentle mixing (200 rpm) at RT, under an argon atmosphere and protected from light. Next, 26.6 nmol of the different oligonucleotide staples (t-1r10f and t-1r4e) carrying a thiol group at the 5′ end was dissolved in 0.1 M triethylamine acetate (TEAAc) solution, mixed with 49 μl of the doxorubicin-EMCS reaction mixture and left to react overnight. The resulting oligonucleotide conjugates were purified by HPLC. The length and homogeneity of the oligonucleotides were determined by MALDI-TOF. The results are shown in Table S2.

Synthesis of the auristatin oligonucleotide conjugate

Staples t-1r20f and t3r20f (26 nmol) carrying thiol groups at the 5′ end was dissolved in 0.1 M TEAAc solution and mixed with 2.8 mM of the maleimide derivative of monomethyl auristatin E (MC-MMAE). The mixture was left to react by gentle mixing at RT overnight. The obtained products were purified and characterized as detailed in Table S2.

Postsynthetic conjugation of folic acid to oligonucleotides

The staples t-3r26e and t1r28f carrying folic acid were prepared by solid-phase conjugation. An amino group was attached to the 5′ end using the N-MMT-6-aminohexyl phosphoramidite. After the addition of the amino linker, the monomethoxytrityl (MMT) group was removed using a standard detritylation solution. Then, 1.2 mg (2.7 μmol) of folic acid was dissolved in 100 μl of anhydrous dimethylformamide (DMF) and activated with 1.4 mg (2.7 μmol) of benzotriazol-1-yloxytripyrrolidinophosphonium hexafluorophosphate (PyBOP) in the

presence of 0.94 μl (5.4 μmol) of diisopropylethylamine (DIEA) for 10 min. Then, this solution was added to 0.2 μmol of 5′-NH_2-oligonucleotide solid support and left to react for 2 h. Finally, the solid support was washed with DMF and acetonitrile (ACN) and dried. The synthetized folic acid staples were purified and characterized as shown in Table S2.

Preparation of DNA origami

Rectangular DNA origami were assembled according the method developed by Rothemund.[2] Modified and unmodified staples were mixed with the M13 scaffold at molar ratio of 5:1:1. DNA origami were annealed and assembled in DNA origami buffer (Tris, 40 mM; Acetic acid, 20 mM; EDTA, 2 mM; and Magnesium acetate, 12.5 mM; pH 8.0) in a thermocycler by slowly cooling from 85 °C to room temperature overnight. The obtained DNA origami were purified using Nanosep 10 K omega (Pall Life Sciences). Finally, the buffer was replaced by a solution of 4 mM $MgCl_2$ in PBS by centrifugation. The final molar concentrations of DNA origami, FdU_{10}, doxorubicin, auristatin, and folic acid used in the experiments are compiled in Table 2.

Agarose gel electrophoresis

DNA origami were analyzed in a 1 % (wt/vol) agarose gel and imaged under UV irradiation. The concentration of DNA nanostructures loaded was 10 nmols in a final volume of 10 μl. The running buffer was 1 × TAE buffer supplemented with 12.5 mM $MgCl_2$ and 5 mM EDTA. Gels were run in a cold room at 4 °C for approximately 50 min at 100 V and stained with SYBR Green. Agarose gels were repeated independently multiple times and consistently yielded same results.

AFM imaging

The different DNA origami were characterized by AFM. Ten microlitres of sample was deposited onto a freshly cleaved mica surface and left to absorb for a short period of time (1–5 min). Then, the sample surface was gently rinsed with buffer to eliminate nonadsorbed DNA. Finally, 60 μl of TAE—Mg^{2+} buffer (40 mM Tris pH 8.0, 12.5 mM Mg^{2+}) was added on the surface, and the different modified DNA origami were visualized in contact mode with MSNL-10 sharpened silicon nitride tips (D cantilever with 225 mm length) with a mean spring constant of 30 pN/nm. Images were processed using Bruker NanoScope Analysis 1.9 software.

Size measurements

The hydrodynamic diameter distribution of the DNA origami modified with FdU_{10}, doxorubicin, auristatin, folic acid and the combination of the four compounds were examined by dynamic light scattering with a DLS with a Zetasizer Nano ZS (Malvern Instruments, Malvern, UK). Every sample in a concentration of 4 nmols in a final volume of 400 μl was measured in duplicate at room temperature and with a detection angle of 173°. All correlation functions were fitted using the cumulant algorithm as implemented in the Malvern software for the calculation of the mean size (average particle size of a population) or *Z*-average and the polydispersity index from the single exponential fitting of the correlation function.

Internalization by flow cytometry

To assess the internalization of DNA origami modified with folic acid, samples were incubated with 1 μl of 1/200 (v/v) SYBRGreen solution in PBS for 1 h at room temperature. A solution of DNA origami buffer incubated with the same SYBR Green solution was used as a negative control. Cells were seeded at a density of 8×10^4 per well in 24-well plates. The next day, the DNA nanostructures were dissolved in fresh growth medium at a final concentration of 2 nM in 500 μl and incubated for 24 h. Then, the cells were washed with PBS, harvested by trypsin treatment, taken up in cell culture medium and centrifuged at 1000 rpm for 5 min. This procedure was repeated twice using PBS, and the remaining supernatant was suspended in 400 μl of cold PBS. Propidium iodide (3 μl) was added before analysis to assess cell viability and exclude dead cells from the flow cytometric internalization analysis. Two independent experiments in duplicate were performed.

Competition studies

Cells were treated with 1 μM folic acid for 40 min. After this, samples at a concentration of 2 nM in 500 μl were added, and the same procedure as that described above was followed. Two independent experiments in duplicate were performed.

Cell viability assay

The cytotoxic activity of the DNA origami loaded with the antitumor drugs (FdU, doxorubicin and auristatin) and folic acid moieties was assessed by the MTT (1-(4,5-dimethylthiazol-2-yl)-3,5-diphenylformazan) assay. After seeding 5×10^3 cells per well in 96-well plates and culturing overnight, the different DNA origami samples were added. Doxorubicin, auristatin, floxuridine, and folic acid were dissolved in sterile 0.5 % (v/v) DMSO in culture medium and plated in the same range of concentrations used for the DNA nanostructures (2 nM for DNA origami and 4 nM for every drug in a final volume of 100 μl). Cells were incubated with samples for 48 h before being washed with PBS. After this time, the MTT reagent was added to each well to a final concentration of 0.5 mg/mL for 3 h of incubation. Absorbance values were measured at 570 nm. Three independent experiments in triplicate were performed.

Internalization pathway studies

Cells were seeded at a density of 8×10^4 per well in 24-well plates. The next day, to inhibit specific endocytic pathway, cells were separately pretreated with 0,25 μM Cytochlasin D (phagocytosis and macropinocytosis) for 15 min, 625 nM Methyl-β-Cyclodextrin (caveolin-dependent endocytosis) for 30 min, or 100 nM sucrose (clathrin-dependent endocytosis) for 30 min. Subsequently, 2 nM of modified DNA origami in a final volume of 500 μl were added for 24 h. Then, the cells were washed with PBS, harvested by trypsin treatment, taken up in cell culture medium and centrifuged at 1000 rpm for 5 min. This procedure was repeated twice using PBS, and the remaining supernatant was suspended in cold PBS. Propidium iodide (3 μl) was added before analysis with flow cytometer. Two independent experiments in duplicate were performed.

Apoptosis assay

The apoptotic cells resulting from exposure to the different treatments were examined by flow cytometry combining fluorescein isothiocyanate (FITC)-Annexin V and propidium iodide. Cells were seeded in 24-well plates with a density of 5×10^4 cells per well. The different modified DNA origami (at a concentration of 2 nM) and drugs (4 nM) in a final volume of 500 μl were then added for 48 h of incubation. The attached cells were harvested with trypsin, and floating cells were washed twice with cold PBS, pelleted and resuspended in Annexin binding buffer plus FITC-Annexin V and propidium iodide according to the manufacturer's specifications. After staining, the samples were analyzed by flow cytometry. Two independent experiments in duplicate were performed.

Fluorescence microscopy

For fluorescence microscopy studies, cells were seeded the day before at a density of 5×10^3 cells per well. Different samples at a concentration of 2 nM and a final volume of 100 μl were then added for 24 h of incubation, and the cells were then washed with PBS. The cells were fixed with 4 % paraformaldehyde, the nuclei were stained using DAPI, and the membrane was stained with WGA-Alexa 555. Images were processed with ImageJ (U. S. National Institutes of Health, Bethesda, Maryland, USA). Two independent experiments in triplicate were performed and the fluorescence microscopy images shown are representative of many acquired images.

Statistical analysis

Statistical analysis was performed by using GraphPad Prism 8 (GraphPad Software, Inc., La Jolla, CA, USA). Quantified data are presented as mean ± SD. One-way ANOVA with the Tukey post hoc test was applied for statistical differences (*$p \leq 0.1$, **$p \leq 0.05$, ***$p \leq 0.01$, **** $p \leq 0.0001$).

Results and discussion

Design, synthesis, and characterization of drug-functionalized staples

Several chemotherapeutic drugs of diverse nature and with different mechanisms of action were selected for its precise incorporation into DNA origami oligonucleotides. To control the exact spatial orientation of drug molecules in DNA nanoscaffolds, an antiproliferative nucleotide (2′-deoxy-5-fluorouridine or floxuridine monophosphate), an intercalating drug (doxorubicin), and an inhibitor of microtubule formation (auristatin) (Fig. 1), were covalently linked to specific structural staples of DNA origami.

In addition, a potential cellular uptake enhancer (folic acid or folate) that has also been previously used in chemotherapy was selected (Fig. 1). To incorporate the different modifications into the DNA origami nanostructures, the molecules needed to be covalently linked to the specific structural staples.

Some time ago, the decanucleotide FdU_{10} was developed by Gmeiner as a prodrug that generates floxuridine monophosphate inside cells after nuclease digestion.[41,42] This is a solution to the cellular resistance observed with 5-fluorouracil (5FU).[43] FdU inhibits both DNA topoisomerase I and thymidylate synthase and has been shown to be more effective than 5-FU in the treatment of cancer.[44] As floxuridine monophosphate is a nucleoside, its incorporation into oligonucleotides is straightforward. Therefore, the solid-phase phosphoramidite methodology used for the assembly of oligonucleotides can be easily adapted for the preparation of oligonucleotides carrying floxuridine.

This strategy was used together with DNA nanostructures reported in a previous article, which indicated that placing the FdU oligomer at the 3′- or 5′ end of the staple is more efficient than locating the FdU oligomer in the loop position of the staple.[9] Accordingly, the FdU decanucleotide sequence was introduced at the 3′ end of the staples (Fig. 1). An amino-controlled pore glass (CPG) solid support was functionalized with 5′-*O*-dimethoxytrityl (DMT)-protected-FdU 3′-hemisuccinate[38] for the synthesis of the FdU_{10} modified staples.

Several methods have been described to chemically link oligonucleotides and drugs.[45] The mechanism of action of the well-known DNA-intercalating drug doxorubicin is inhibition of DNA topoisomerase II, but doxorubicin also affects other cellular processes through the generation of reactive oxygen species (ROS) or DNA intercalation, causing DNA damage and inducing apoptosis.[46] The ability of doxorubicin to intercalate with DNA and the large number of studies on this drug have positioned it as the gold standard in terms of chemotherapeutic drugs that can be loaded into DNA nanostructures. However, this method has several drawbacks (e.g., every approach has its own, different loading and purification strategies, environment, and pH), making it challenging to compare the results obtained between studies. For that reason, we decided to covalently conjugate doxorubicin to two staples.

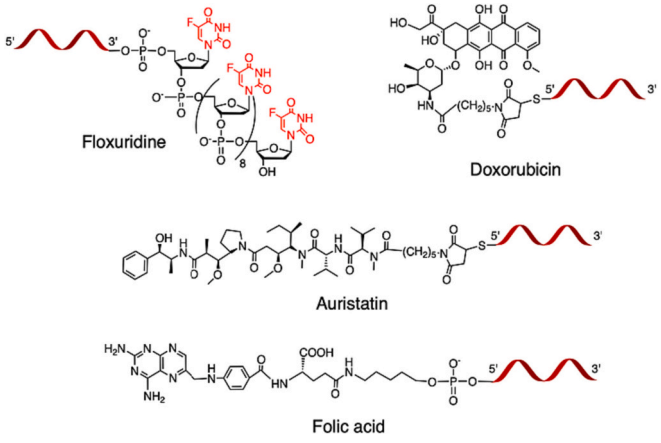

Fig. 1. Schematic representation of the modified staples. FdU_{10}, auristatin, and doxorubicin were incorporated into structural staples via different synthetic strategies to function as chemotherapeutic drugs. Folic acid was incorporated at the 5′ end of the oligonucleotide to act as a cellular uptake enhancer.

Doxorubicin has a primary amino group that can be used to form amide bonds, but the introduction and activation of carboxylic groups into oligonucleotides is not very efficient. For this reason, we selected a bifunctional crosslinker that carries both maleimide and N-hydroxysuccinimidyl ester groups. For this purpose, the maleimide-doxorubicin intermediate was first generated by covalently linking the bifunctional crosslinker to doxorubicin. Then, the maleimide doxorubicin intermediate was reacted with 5′-thiolated oligonucleotide staples in solution to generate the doxorubicin conjugates (Figs. S1A, S2).

On the other hand, despite extensive research on DNA nanostructures for therapeutics, the type of drug molecules that can be loaded into them is limited to few drugs with the ability to intercalate DNA, which limits the potential of DNA nanoscaffolds as drug delivery vehicles. For that reason, to expand the scope of drug molecules that can be incorporated into DNA origami, auristatin-oligonucleotide conjugates were prepared. Auristatin is a potent derivative of the natural product dolastatin 10 that induces apoptosis by inhibiting tubulin polymerization in dividing cells.[47] The synthesis of oligonucleotide-auristatin conjugates was performed by a direct reaction between commercially available maleimide-auristatin and 5′-thiolated oligonucleotide staples (Fig. S1B).

The synthesis of folate-oligonucleotide conjugates has been previously described.[48] We selected this strategy based on the formation of an amide bond between the 5′-aminohexyl-oligonucleotide and folic acid while the assembled oligonucleotide was still attached to the solid support. The reaction between the solid-phase supported amino-oligonucleotide and folic acid was performed using an excess of folic acid activated with PyBOP in an anhydrous organic solvent (Fig. S1C).

In all cases, the expected conjugates (Table S1) were obtained as the major products as determined by reverse-phase HPLC (Figs. S3, S4, S5, S6) analysis and purified. The identities of the purified conjugates were confirmed by MALDI-TOF (Table S2).

Preparation and characterization of DNA origami

A series of DNA origami nanostructures were prepared by hybridization of unmodified staples as well as appropriate modified staples carrying doxorubicin, auristatin, and/or FdU_{10} (Table 1). These nanostructures were also assembled with modified staples carrying folic acid

Table 1
Modified staples of the engineered DNA origami.

Sample	Drug staples	Folate staples
Origami-FdU_{10}-Folic	t-3r8e-FdU_{10}, t3r6f-FdU_{10}	Fol-t-3r26e, Fol-t1r28f
Origami-Dox-Folic	Dox-t-1r10f, Dox-t-1r14e	Fol-t-3r26e, Fol-t1r28f
Origami-Aur-Folic	Aur-t-1r20f, Aur-t3r26e	Fol-t-3r26e, Fol-t1r28f
Origami fully modified	t-3r8e-FdU_{10}, t3r6f-FdU_{10}, Dox-t-1r10f, Dox-t-1r14e, Aur-t-1r20f, Aur-t3r26e	Fol-t-3r26e, Fol-t1r28f

to facilitate their internalization. A schematic representation of the specific positioning of the functionalized staples (Table 1) inserted into the rectangular DNA origami is shown in Fig. 2A.

The rectangular DNA origami nanostructures were assembled by hybridization of the M13 DNA scaffold and the appropriate staple strands using the single-step method reported by Rothemund.[2] The nanostructures were subsequently characterized before and after the incorporation of the different modified staples by agarose gel electrophoresis, dynamic light scattering (DLS) and atomic force microscopy (AFM). As shown in the agarose gel electrophoresis images (Figs. 2B and S7), all of the modified DNA origami appeared as single bands with slightly slower mobility than the corresponding M13 scaffold, indicating the absence of potential aggregations. Although the resolution of AFM does not enable the visualization of individual drug molecules, due to their small sizes, the rectangular morphology of the DNA origami was maintained after incorporation of the extended staples with each drug (doxorubicin, auristatin, and FdU_{10}) either alone or in combination with folic acid, as clearly observed in the AFM images (Figs. 2C, S8, S9). The DLS measurements demonstrated that each one of the small molecules do not alter much the hydrodynamic size of the DNA nanostructures, when incorporated individually. However, an increase in the size was observed on the fully modified DNA origami (Table S3 and Fig. S10). These results unambiguously confirmed the formation of DNA origami carrying the selected drugs with the expected size and shape.

Folate as a cellular uptake enhancer

Folic acid has been described to bind to folate receptors, which are highly overexpressed on the surface of several tumor cells, including colorectal cancer cells.[36,37] Therefore, to facilitate the internalization of the DNA nanoscaffolds, folic acid was incorporated into DNA origami nanostructures to potentially enhance cellular uptake. First, we studied the cellular uptake of DNA origami modified with two folic acid-modified staples in two different colorectal cancer cell lines: HTB38 and HCC2998 cells. For this purpose, we carried out flow cytometry by intercalating SYBR Green into the prepared DNA origami and fluorescence imaging-based measurements by incorporating fluorescein (FAM)-modified staples into the rectangular DNA origami. As shown in Fig. 3, the intensity of the fluorescence signal inside the cells was larger when DNA origami was modified with two folate moieties. The fluorescence microscopy measurements in Fig. 4A and B verified the flow cytometry results, clearly indicating that cells that were not treated or treated with unmodified origami had no observable or very low fluorescence and confirming that intracellular fluorescence intensity was significantly higher when the DNA origami incorporated folic acid. The images also show that the fluorescence signals are predominantly localized in the cytoplasm, as confirmed after staining the nuclei with DAPI and the cellular membrane with WGA555. The nonuniform distribution of the fluorescence in the cytoplasm may be attributed to the DNA origami being confined in specific organelles such as endosomes or lysosomes.[49,50]

Moreover, when comparing HTB38 and HCC2998 cells, it was noticed that more folic acid-modified DNA origami was internalized by HCC2998 cells. A competition study was performed to assess the involvement of folic acid and FOLR1 receptors in the uptake of folic acid-modified DNA origami in the HTB38 and HCC2998 cell lines. Folic acid was used to competitively bind to and saturate the folate receptors and thus minimize accessibility to the modified DNA origami. In both cell lines, flow cytometry showed a reduction in uptake by the cells treated with folic acid compared to nontreated cells (Fig. 4C), indicating that FOLR1 is responsible for the uptake of folic acid-modified DNA origami by both HTB38 and HCC2998 cells. Surprisingly, in HTB38 cells, folic acid was not capable of completely blocking the entry of the modified DNA origami. The FOLR1 expression levels were also examined in both cell lines by flow cytometry and fluorescence imaging analyses using a PE-labeled FOLR1 primary antibody. The studies revealed

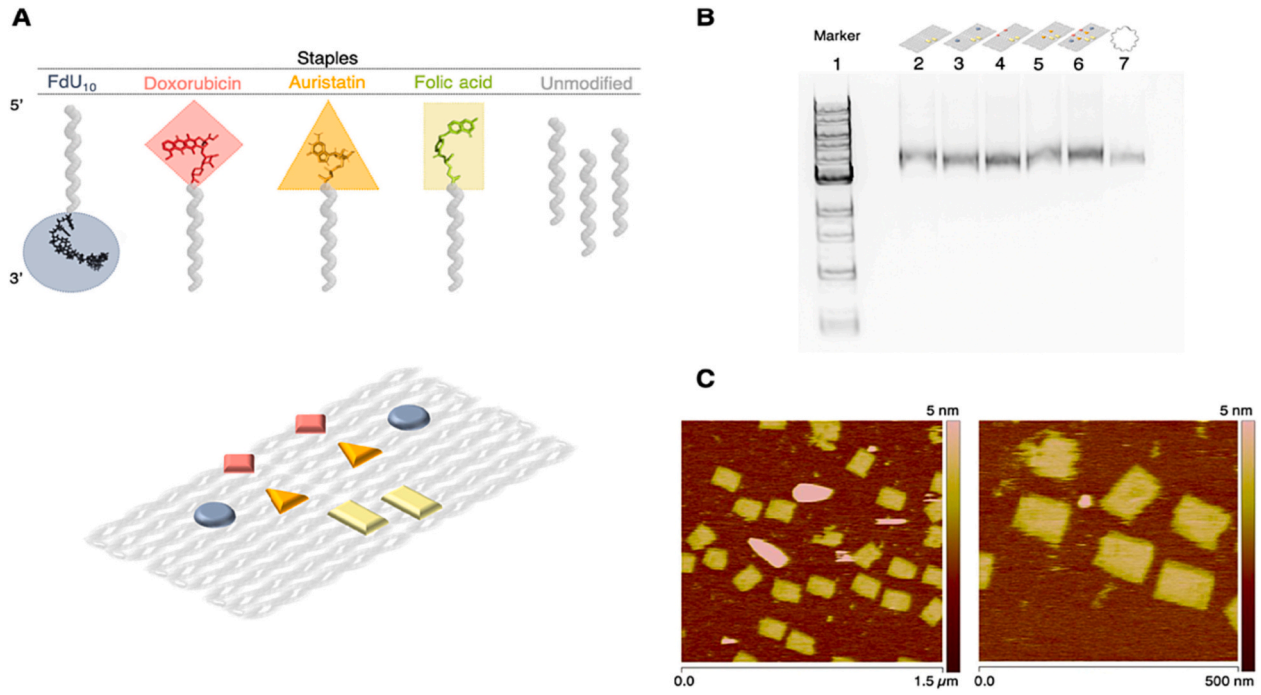

Fig. 2. Schematic representation of the design, construction, and characterization of the DNA origami. A) Process of DNA origami assembly with the modified and unmodified staples. Rectangular DNA origami is represented in grey, while the modified staples with doxorubicin, auristatin, FdU_{10}, and folic acid are shown in red, orange, blue, and green, respectively. B) Agarose gel electrophoresis (1 %) of purified DNA origami nanostructures: (1) 1 kb ladder, (2) DNA origami modified with folate, (3) DNA origami carrying folate and FdU_{10}, (4) DNA origami modified with folate and doxorubicin, (5) DNA origami carrying folate and auristatin, (6) fully modified DNA origami (folate, FdU_{10}, doxorubicin, and auristatin), and (7) M13 DNA scaffold. C) AFM images of the fully modified DNA origami confirming the expected rectangular shape. The illustrations in the figure are not to scale.

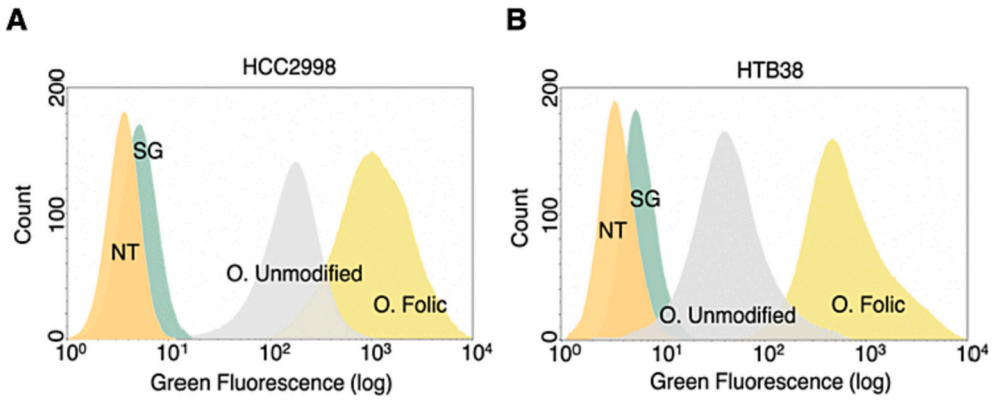

Fig. 3. Flow cytometry analysis of the uptake of unmodified DNA origami and folic acid-modified DNA origami by A) HCC2998 and B) HTB38. Nontreated (NT) and SYBR Green (SG) solution-treated cells were included as negative controls.

that both cell lines express FOLR1, but HCC2998 cells have relatively higher levels of folate receptor expression than HTB38 cells (Fig. S11). These results are in good agreement with the flow cytometry and microscopy studies showing that the higher the expression levels of FOLR1 are, the higher the amount of folic acid-modified DNA origami internalized. Having observed that proposed DNA origami exhibited different cell entry capability, we further proceeded to investigate their endocytic pathways.[51] Endocytosis can follow diverse mechanisms and for that reason inhibitors of different endocytic pathways were used: Cytochalasin D (actin polymerization),[52] methyl-beta-cyclodextrin (caveolin-mediated endocytosis),[53] and sucrose (clathrin-mediated endocytosis).[54] On one hand, DNA origami transfected with Lipofectamine is not very affected by inhibitors indicating that it may follow other mechanisms of internalization. Unmodified DNA origami have similar behaviors in both cell lines with higher inhibition by sucrose indicating a clathrin-mediated endocytosis. On the other hand, DNA origami modified with folic acid are internalized following different endocytic pathways depending on the colorectal cancer cell type (clathrin-mediated in HTB38 and caveolin-mediated in HCC2998). These findings (Fig. 5) are in concordance with Rajwar et al. that reported a cell type dependence of the endocytosis mechanism of DNA nanostructures.[55] Interestingly, in the HCC2998 cell line, folate DNA origami follows a caveolin-mediated endocytosis in good agreement with previous studies that revealed that ligands such as albumin, cholesterol or folic acid can be internalized following this pathway.[56]

Antitumor activity of the multifunctionalized DNA origami

The cytotoxicity of multifunctional DNA origami nanostructures with folate-mediated endocytosis or transfected with Lipofectamine was evaluated in HTB38 and HCC2998 cancer cells. These data were compared to those of the free drugs, doxorubicin, auristatin, and FdU_{10}, as well as drug-modified staples transfected with Lipofectamine (Fig. 6). Folic acid-modified and unmodified DNA origami were used as negative controls (Fig. S12). As shown in Table 2, concentrations of the free drug and the drug conjugated to the staple were the same as the final concentration of drug loaded into the DNA origami (4 nM doxorubicin, 4 nM auristatin, and 40 nM FdU_{10}).

In regard to the obtained results from the HCC2998 cell line and considering cellular viability, doxorubicin seemed to have the highest cytotoxic activity when compared with the other drugs. Moreover, the cellular viability percentage indicated that HCC2998 cells are fairly resistant to FdU_{10}, which is in good agreement with previous studies.[9] The same experiments were conducted with DNA origami modified with the drugs and with and without folate. For all drugs, improved drug activity was observed when the DNA origami nanostructure incorporated folate, which enhances cellular uptake. Furthermore, the collected data show similar behavior to the viability results after the cells were treated with free drug, with the DNA origami loaded with doxorubicin having the highest cytotoxic effect, followed by the DNA origami modified with auristatin. Interestingly, when doxorubicin was incorporated into the DNA origami by covalent conjugation to the staples, the drug was more cytotoxic that when it was loaded by intercalation, which was achieved by incubating the DNA nanostructure with the same concentration of drug. This fact may show the impossibility of unambiguously quantifying the properties of the DNA origami intercalated with doxorubicin.

Overall, the lowest cellular viability percentages were obtained after transfection with Lipofectamine, with a reduction of cellular viability of up to 25 % compared to that of DNA origami without the incorporation of any cellular uptake enhancer.

On the other hand, HTB38 cells displayed different activity after treatment with DNA origami. The abovementioned colorectal cancer cells seem to be more sensitive to auristatin when incubated with the free drug or the DNA origami loaded with auristatin, both of which resulted in higher cytotoxicity. Moreover, compared to HCC2998 cells, FdU_{10} had higher activity in HTB38 cells, which is in good agreement with previously reports suggesting the higher sensitivity of this cell line to FdU.[9] However, in accordance with the data from HCC2998 cells, the cellular viability decreased when either folic acid or Lipofectamine were incorporated into the DNA origami loaded with the different drugs, thus confirming the potential of using folic acid as a tumor cell internalization enhancer and the good cytotoxic activity of the proposed chemotherapeutic DNA origami.

Finally, taking advantage of the large number of positions in the rectangular DNA origami that can be functionalized, all of the drugs were incorporated in the same nanostructure with further modification with folic acid or transfection with Lipofectamine. Although the functionalization of DNA origami with folate improved the cytotoxicity of the modified DNA origami in both cell lines, the most interesting results came from transfection of the multifunctionalized DNA origami with Lipofectamine, which reduced cellular viability by approximately 60 %. Moreover, these results show a synergetic effect when several drugs with different action mechanisms are present, indicating that the incorporation of more than one type of chemotherapeutic drug may be a potential solution for urgent clinical needs such as drug resistance. The uptake and cytotoxicity of the DNA origami nanostructures have also been studied in HeLa cells (Figs. S13 and S14) showing a similar behavior than in the studied colorectal cancer cells. All in all, the drug-staples transfected with Lipofectamine and the free drug controls exhibit very low toxicities, likely due to distinct internalization mechanisms. On one hand, free drug molecules are typically internalized through diffusion, whereas the drug-oligonucleotide conjugates transfected with Lipofectamine are taken up by cells through alternative processes. Importantly, for all three drugs, their incorporation into DNA nanostructures enhances cytotoxicity, indicating that the DNA origami substrate

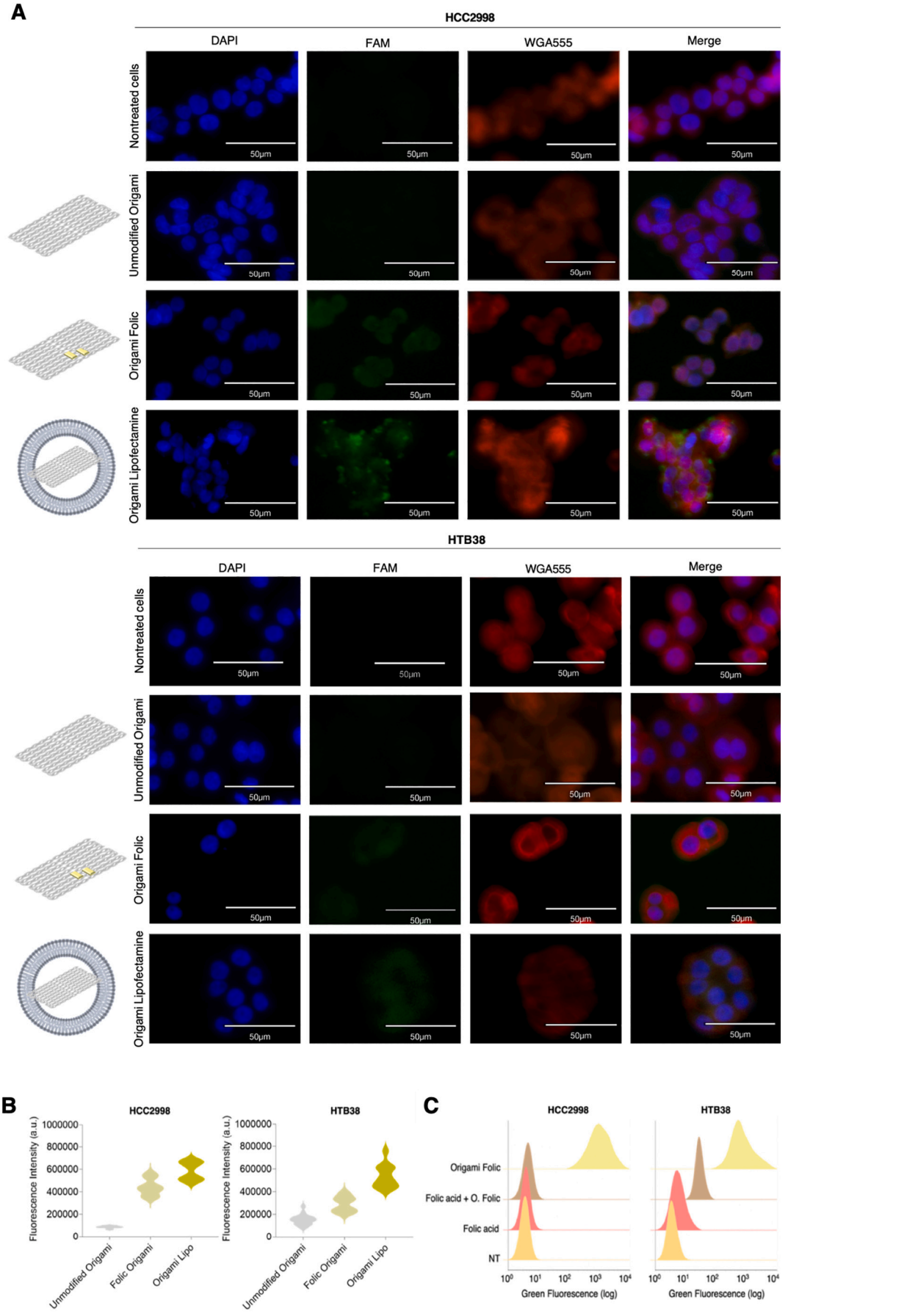

(caption on next page)

Fig. 4. Cellular uptake study of DNA origami by HCC2998 and HTB38 cells. A) Representative fluorescence microscopy images of DNA origami in HCC2998 and HTB38 cells after 24 h of incubation. Strong FAM fluorescence in the cytoplasm was observed in cells treated with folic acid-modified DNA origami but not for the nontreated cells or those treated with bare DNA origami. B) FAM fluorescence intensities of the different DNA origami structures. DNA origami transfected with Lipofectamine (Lipo) was included as a positive control. C) Uptake of folic acid-modified DNA origami by both cell lines after inhibition of FOLR1. Significant inhibition of folate DNA origami uptake by both cell lines was observed for cells treated with folic acid (94 % reduction by HCC2998 cells and 78 % by HTB38 cells) since folic acid binds to and saturates FOLR1 to block accessibility for the folate-functionalized DNA origami. The illustrations in the figure are not to scale.

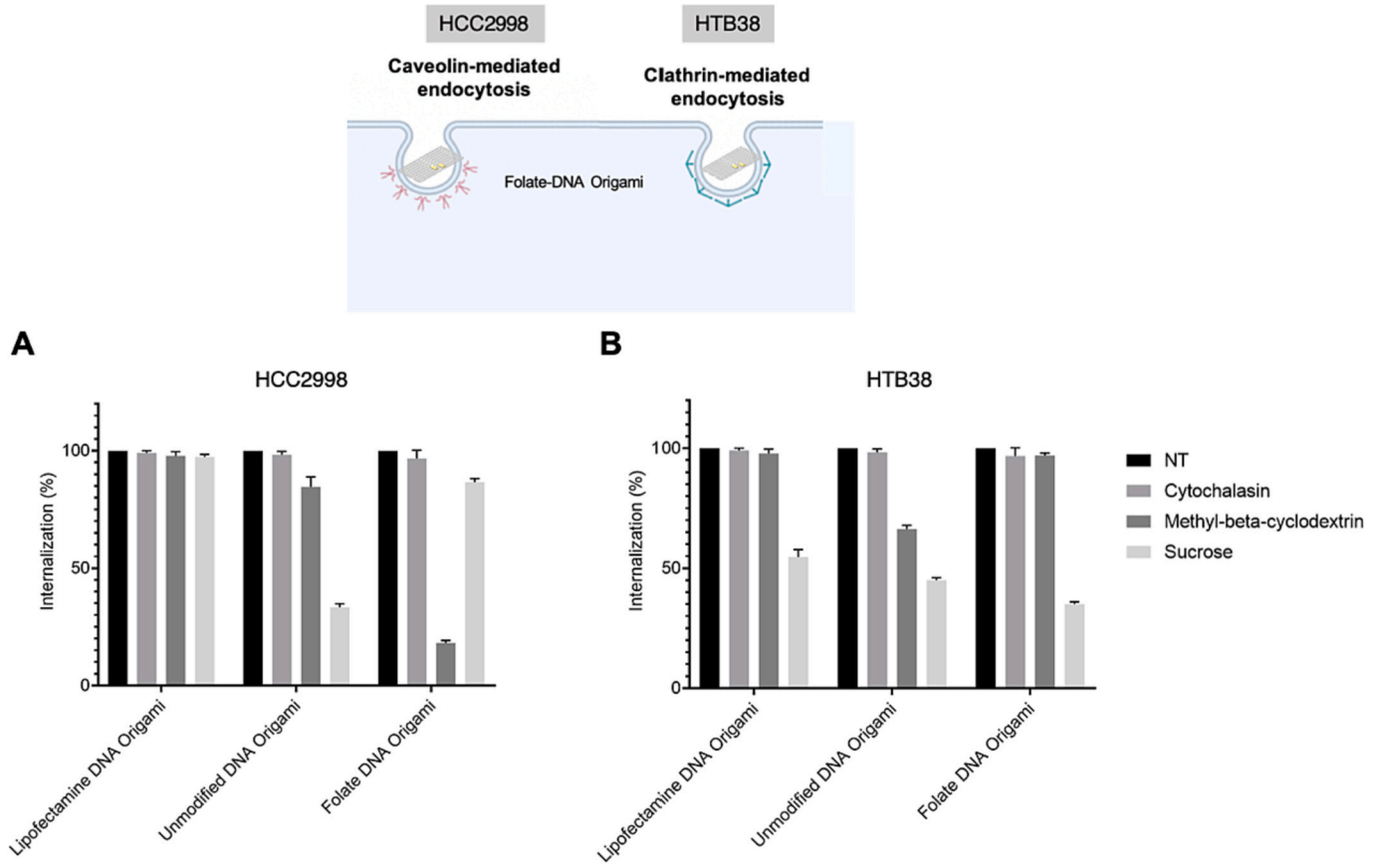

Fig. 5. Endocytosis pathways in colorectal cancer cells. Histogram analysis of the fluorescence signal of A) HCC2998 and B) HTB38 cell lines treated with unmodified DNA origami, folate-DNA origami, and DNA origami transfected with Lipofectamine (Lipo) in the presence of different endocytic inhibitors (shown in the legend). The relative cellular uptake efficiency was calculated by setting the signal of the cells treated with corresponding DNA origami in nontreated conditions (NT) as 100 %.

enhances drug efficiency. The apoptosis assay results (Fig. 7) are in good agreement with the cytotoxicity results from the MTT assay, thus validating the consistency of our data, with the exception of the fully modified DNA origami with folate in HCC2998 cells. DNA nanostructures carrying FdU_{10} and transfected with Lipofectamine promoted less apoptosis of HCC2998 cells than HTB38 cells, consistent with previous studies related to resistance to FdU. Similar cellular damage was observed with DNA origami carrying auristatin or doxorubicin in both cell lines when the DNA origami were modified with folate. In both cell lines, greater cell damage was noted when the modified DNA nanostructures were transfected with Lipofectamine. Moreover, the transfected DNA nanostructures showed a greater tendency to induce necrosis. These findings suggest that the uptake mechanism plays a role in the apoptosis process, as folate DNA nanostructures induce apoptosis, while DNA origami transfected with Lipofectamine promotes an increase in necrosis in both cell lines. In addition, the fully modified DNA origami more efficiently promoted apoptosis than the DNA origami nanostructures carrying only one type of drug. This finding confirms a synergy resulting from the incorporation of three different antitumor drugs. We believe that the cytotoxic effect of DNA origami with the three drugs and folate paves a new avenue towards the design of targeted, multifunctionalized DNA nanostructures for therapeutic purposes.

Discussion

In this work, we demonstrate how antitumor drugs of different natures can be covalently linked to structural staples, simplifying the preparation of defined multifunctionalized DNA origami nanostructures and avoiding the large number of drawbacks observed when noncovalent strategies are used, such as competition for various binding sites, limited accessibility, an unknown number of drug-DNA binding events or undesired toxicity.[12]

To the best of our knowledge, our findings represent the first evidence that doxorubicin can be precisely incorporated into DNA nanostructures. DNA origami carrying covalently attached doxorubicin exhibit high cytotoxicity, whereas the functionalized staples alone are less toxic. Furthermore, this is the first time that auristatin has been incorporated into DNA nanostructures and demonstrated high cytotoxicity to the studied HTB38 and HCC2998 cells. Therefore, having improved the ability of DNA origami to function as a chemotherapeutic molecule delivery vehicle by covalent binding of the drug to structural staples and control the precise concentration of drugs, we truly believe

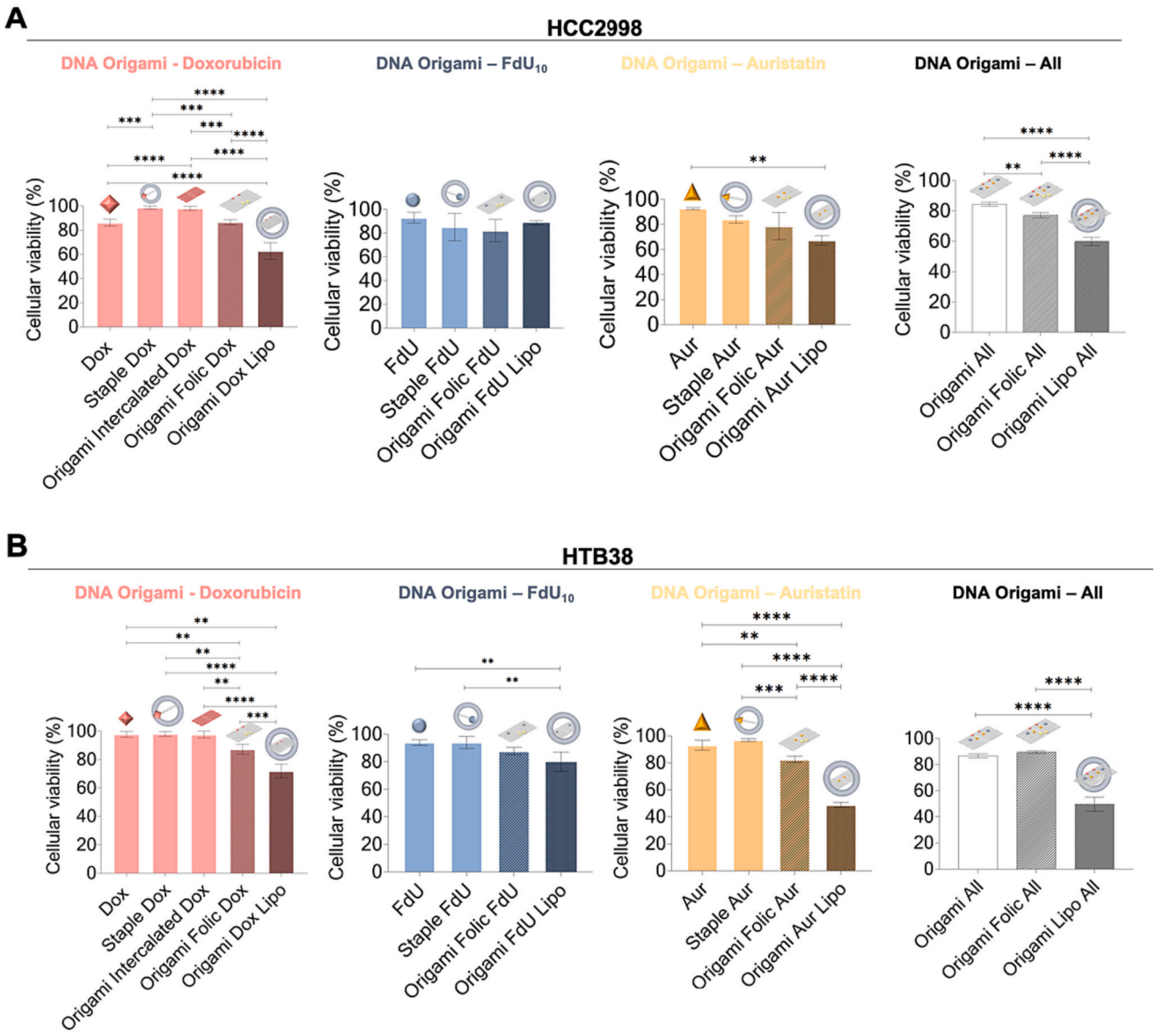

Fig. 6. Cytotoxicity of DNA origami nanostructures determined by MTT assay. Cells were treated with modified DNA origami, and the results were compared to those after treatment with the free drugs and drug-conjugated staples transfected with Lipofectamine: A) HCC2998 cells and B) HTB38 cells. Error bars represent standard deviation (SD) of three independent experiments in triplicate. One-way ANOVA with the Tukey post hoc test was applied for statistical differences (*$p \leq 0.1$, **$p \leq 0.05$, ***$p \leq 0.01$, **** $p \leq 0.0001$). The illustrations in the figure are not to scale.

Table 2
Number of modified staples, concentration of DNA origami, and their respective total concentration of incorporated drugs.

Sample	Number of modified staples	Molar concentration of DNA nanoscaffold (nM)	Total concentration of drug (nM)
Origami-Folic	2	2	4
Origami-FdU_{10}	2	2	4[a]
Origami-Dox	2	2	4
Origami-Aur	2	2	4

[a] Refering to the decamer FdU_{10}.

that this achievement sheds light on the speculations generated from the ambiguous results of previous studies on DNA nanostructures as drug delivery vehicles with noncovalently incorporated drugs for chemotherapeutic purposes.

Furthermore, as a proof of concept, we show rectangular DNA origami as a potential vehicle for several types of drug molecules, even those that cannot be intercalated but are widely used as therapeutic compounds, thus expanding the scope of drugs that can be precisely loaded on DNA nanostructures. Significantly, the multifunctionalized DNA origami exhibits cytotoxicity at nanomolar concentrations, surpassing that of the clinical reference drugs and even the functionalized drug-staple conjugates. While the typical dosage of cancer treatment drugs varies widely based on the cancer type, specific drug used, disease stage, and individual patient characteristics, it's important to note that conventional chemotherapy often involves the systemic administration of cytotoxic drugs at relatively high doses. These drugs are distributed throughout the body and can impact both cancerous and healthy cells. Furthermore, conventional drugs lack specific targeting mechanisms for

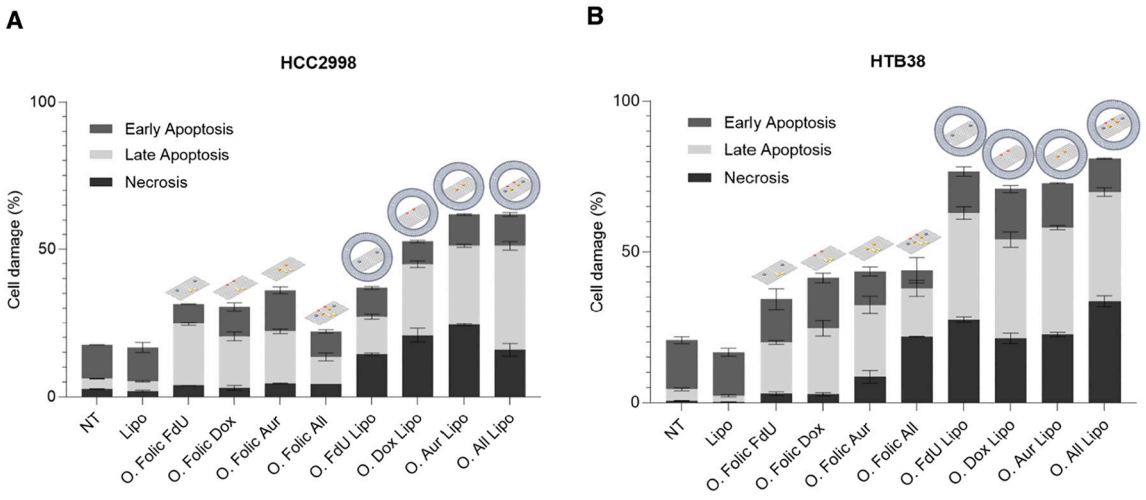

Fig. 7. Apoptosis assays comparing folate-modified DNA nanostructures and DNA origami transfected with Lipofectamine in A) HCC2998 and B) HTB38 cells. Nontreated (NT) and Lipofectamine (Lipo) solution-treated cells were included as negative controls. Error bars represent standard deviation (SD) of two independent experiments in duplicate. The illustrations in the figure are not to scale.

cancer cells, leading to the destruction of not only cancer cells but also healthy.[57] In contrast, DNA nanostructures can be engineered to transport drugs directly to cancer cells and tumor tissues,[58] allowing for concentrated drug delivery at the intended site. This targeted delivery enables the use of lower drug doses, thereby minimizing exposure to healthy tissues and potentially reducing the severity of side effects associated with cancer treatment. Lower doses also imply fewer adverse effects on the overall health of the patient. A critical aspect is that DNA origami can be tailored for controlled and sustained drug release, ensuring the maintenance of therapeutic drug concentrations at the tumor site over time and reducing the need for high initial doses. Similarly, our work demonstrates that these structures can simultaneously deliver multiple drugs with distinct mechanisms of action, thereby enhancing treatment efficacy without a significant increase in the overall drug dosage. However, it is important to note that the dosage of drugs delivered using DNA nanostructures still depends on the specific drug, the design of the nanostructures, and the desired treatment outcome.[59]

Furthermore, we believe that the unprecedented control over the exact concentration of drugs per DNA origami, presented here, could become more cost-efficient and scalable compared to current methods that rely on drug intercalation.

Undoubtedly, there is still plenty of room to improve DNA nanostructures for therapeutic applications. For instance, it would be of interest to explore DNA origami with diverse shapes, investigate the impact of different positioning of drug-staple conjugates, and determine the optimal number of modified drug-staples within each DNA nanocarrier. These, can serve as future steps for advancing the approach proposed here.

Another crucial aspect is the finding of a targeting molecule that not only acts as an enhancer of cellular uptake but also can selectively bind to specific tumor cells, as it will decrease off-target effects and increase the overall potential. Nevertheless, we believe that the development of the multifunctionalized DNA origami is a step forwards and paves new avenues in the engineering of DNA nanostructures with precise contents and architecture for use as chemotherapeutic drug delivery vehicles.

Conclusion

In conclusion, we demonstrate the incorporation of well-known antitumor drugs, including doxorubicin, auristatin, and floxuridine, into DNA nanostructures through covalent linking to structural staples. This method effectively addresses concerns related to the unpredictability of drug-DNA binding interactions and premature drug release.

Furthermore, the covalently modified DNA origami approach allows for precise integration of multiple synergistic antitumor drugs at predetermined molar ratios and facilitates controlled spatial orientation within the DNA structure.

The findings underscore a pioneering and distinct methodology for the development of DNA nanostructures as efficient vehicles for targeted drug delivery, marking a significant stride towards the realization of precise and effective nanomedicines for cancer treatment.

CRediT authorship contribution statement

Natalia Navarro and Carme Fàbrega contributed equally to this work. Òscar Domènech and Jordi H. Borrell: AFM images. Anna Aviñó: chemical synthesis, writing-review and editing. Natalia Navarro: synthesis and characterization of DNA origami, biological assays, visualization, formal analysis, figure preparation, writing-original draft, writing-review and editing. Ramon Eritja: conceptualization, writing-original draft, writing-review and editing, supervision, funding acquisition. Carme Fàbrega: chemical synthesis, synthesis and characterization of DNA origami, biological assays, visualization, formal analysis, figure preparation, writing-original draft, writing-review and editing, supervision, funding acquisition. All authors have read and agreed to the published version of the manuscript.

Funding

This work was financially supported by the Spanish Ministerio de Ciencia e Innovación (MICINN) (Project CTQ2017-84415-R and PID2020-118145RB-I00), Explora project (CTQ2014-61758-EXP and BIO2017-92113-EXP) and 7th Framework Programme (NMP2007-213382, NMP-LA-2011-262943, COST Action CA17103). N.N. held a predoctoral contract grant (PRE2021-097856). CIBER-BBN is an initiative funded by the VI National R + D + I Plan 2008–2011, Iniciativa Ingenio 2010, Consolider Program, CIBER Actions and financed by the Instituto de Salud Carlos III with assistance from the European Regional Development.

Declaration of competing interest

The authors declare that they have no known competing financial interests or personal relationships that could have appeared to influence

the work reported in this paper.

Data availability

The data are available from the corresponding authors () on reasonable request.

Acknowledgments

We acknowledge Dra. Susana Vilchez and ICTS NANBIOSIS (U12) for technical advice and support to DLS experiments and Dr. Ramon Mangues for kindly providing us Auristatin maleimide. We also thank ICTS NANBIOSIS (Oligonucleotide synthesis platform U29).

Appendix A. Supplementary data

Supplementary data to this article can be found online at https://doi.org/10.1016/j.nano.2023.102722.

References

1. Seeman NC. Nucleic acid junctions and lattices. *J Theor Biol*. 1982;99:237–247. https://doi.org/10.1016/0022-5193(82)90002-9.
2.. Rothemund PWK. Folding DNA to create nanoscale shapes and patterns. *Nature*. 2006;440:297–302. https://doi.org/10.1038/nature04586.
3. Yang Q, Chang X, Lee JY, Olivera TR, Saji M, Wisniewski H, et al. Recent advances in self-assembled DNA nanostructures for bioimaging. *ACS Appl Bio Mater*. 2022. https://doi.org/10.1021/acsabm.2c00128.
4. Dey S, Fan C, Gothelf KV, Li J, Lin C, Liu L, et al. DNA origami. *Nat Rev Methods Primers*. 2021;1:13. https://doi.org/10.1038/s43586-020-00009-8.
5. Tintoré M, Gállego I, Manning B, Eritja R, Fàbrega C. DNA origami as a DNA repair nanosensor at the single-molecule level. *Angew Chem*. 2013;125:7901–7904. https://doi.org/10.1002/ange.201301293.
6.. Wang S, Zhou Z, Ma N, Yang S, Li K, Teng C, et al. DNA origami-enabled biosensors. *Sensors*. 2020;20:6899. https://doi.org/10.3390/s20236899.
7. Gállego I, Manning B, Prades JD, Mir M, Samitier J, Eritja R. DNA-origami-driven lithography for patterning on gold surfaces with sub-10 nm resolution. *Adv Mater*. 2017;29, 1603233. https://doi.org/10.1002/adma.201603233.
8. Yang Y, Zhang R, Fan C. Shaping functional materials with DNA frameworks. *Trends Chem*. 2020;2:137–147. https://doi.org/10.1016/j.trechm.2019.11.005.
9.. Jorge AF, Aviñó A, Pais AACC, Eritja R, Fàbrega C. DNA-based nanoscaffolds as vehicles for 5-fluoro-2′-deoxyuridine oligomers in colorectal cancer therapy. *Nanoscale*. 2018;10:7238–7249. https://doi.org/10.1039/C7NR08442K.
10. Weiden J, Bastings MMC. DNA origami nanostructures for controlled therapeutic drug delivery. *Curr Opin Colloid Interface Sci*. 2021;52, 101411. https://doi.org/10.1016/j.cocis.2020.101411.
11.. Seeman NC, Sleiman HF. DNA nanotechnology. *Nat Rev Mater*. 2017;3:17068. https://doi.org/10.1038/natrevmats.2017.68.
12. Keller A, Linko V. Challenges and perspectives of DNA nanostructures in biomedicine. *Angew Chem Int Ed*. 2020;59:15818–15833. https://doi.org/10.1002/anie.201916390.
13. Lacroix A, Sleiman HF, Nanostructures DNA. Current challenges and opportunities for cellular delivery. *ACS Nano*. 2021;15:3631–3645. https://doi.org/10.1021/acsnano.0c06136.
14. Knappe GA, Wamhoff E-C, Bathe M. Functionalizing DNA origami to investigate and interact with biological systems. *Nat Rev Mater*. 2022. https://doi.org/10.1038/s41578-022-00517-x.
15. Ma W, Zhan Y, Zhang Y, Shao X, Xie X, Mao C, et al. An intelligent DNA nanorobot with in vitro enhanced protein lysosomal degradation of HER2. *Nano Lett*. 2019;19:4505–4517. https://doi.org/10.1021/acs.nanolett.9b01320.
16. Schaffert DH, Okholm AH, Sørensen RS, Nielsen JS, Tørring T, Rosen CB, et al. Intracellular delivery of a planar DNA origami structure by the transferrin-receptor internalization pathway. *Small*. 2016;12:2634–2640. https://doi.org/10.1002/smll.201503934.
17. Li S, Jiang Q, Liu S, Zhang Y, Tian Y, Song C, et al. A DNA nanorobot functions as a cancer therapeutic in response to a molecular trigger in vivo. *Nat Biotechnol*. 2018;36:258–264. https://doi.org/10.1038/nbt.4071.
18. Zhang H, Demirer GS, Zhang H, Ye T, Goh NS, Aditham AJ, et al. DNA nanostructures coordinate gene silencing in mature plants. *Proc Natl Acad Sci*. 2019;116:7543–7548. https://doi.org/10.1073/pnas.1818290116.
19. Nicolson F, Ali A, Kircher MF, Pal S. DNA nanostructures and DNA-functionalized nanoparticles for cancer theranostics. *Adv Sci*. 2020;7:2001669. https://doi.org/10.1002/advs.202001669.
20. Halley PD, Lucas CR, McWilliams EM, Webber MJ, Patton RA, Kural Comert, et al. Daunorubicin-loaded DNA origami nanostructures circumvent drug-resistance mechanisms in a leukemia model. *Small*. 2016;12:308–320. https://doi.org/10.1002/smll.201502118.
21. Zhao Y-X, Shaw A, Zeng X, Benson E, Nyström AM, Högberg B. DNA origami delivery system for cancer therapy with tunable release properties. *ACS Nano*. 2012;6:8684–8691. https://doi.org/10.1021/nn3022662.
22. Kollmann F, Ramakrishnan S, Shen B, Grundmeier G, Kostiainen MA, Linko V, et al. Superstructure-dependent loading of DNA origami nanostructures with a groove-binding drug. *ACS Omega*. 2018;3:9441–9448. https://doi.org/10.1021/acsomega.8b00934.
23.. Xie X, Shao X, Ma W, Zhao D, Shi S, Li Q, et al. Overcoming drug-resistant lung cancer by paclitaxel loaded tetrahedral DNA nanostructures. *Nanoscale*. 2018;10:5457–5465. https://doi.org/10.1039/C7NR09692E.
24.. Ge Z, Guo L, Wu G, Li J, Sun Y, Hou Y, et al. DNA origami-enabled engineering of ligand–drug conjugates for targeted drug delivery. *Small*. 2020;16, 1904857. https://doi.org/10.1002/smll.201904857.
25. Wiraja C, Zhu Y, Lio DCS, Yeo DC, Xie M, Fang W, et al. Framework nucleic acids as programmable carrier for transdermal drug delivery. *Nat Commun*. 2019;10:1147. https://doi.org/10.1038/s41467-019-09029-9.
26. Pan Q, Nie C, Hu Y, Yi J, Liu C, Zhang J, et al. Aptamer-functionalized DNA origami for targeted codelivery of antisense oligonucleotides and doxorubicin to enhance therapy in drug-resistant cancer cells. *ACS Appl Mater Interfaces*. 2020;12:400–409. https://doi.org/10.1021/acsami.9b20707.
27. Liu J, Song L, Liu S, Jiang Q, Liu Q, Li N, et al. A DNA-based Nanocarrier for efficient gene delivery and combined Cancer therapy. *Nano Lett*. 2018;18:3328–3334. https://doi.org/10.1021/acs.nanolett.7b04812.
28.. Zeng Y, Nixon RL, Liu W, Wang R. The applications of functionalized DNA nanostructures in bioimaging and cancer therapy. *Biomaterials*. 2021;268, 120560. https://doi.org/10.1016/j.biomaterials.2020.120560.
29. Jiang Q, Song C, Nangreave J, Liu X, Lin L, Qiu D, et al. DNA origami as a carrier for circumvention of drug resistance. *J Am Chem Soc*. 2012;134:13396–13403. https://doi.org/10.1021/ja304263n.
30. Zhang Q, Jiang Q, Li N, Dai L, Liu Q, Song L, et al. DNA origami as an *in vivo* drug delivery vehicle for cancer therapy. *ACS Nano*. 2014;8:6633–6643. https://doi.org/10.1021/nn502058j.
31. Ijäs H, Shen B, Heuer-Jungemann A, Keller A, Kostiainen MA, Liedl T, et al. Unraveling the interaction between doxorubicin and DNA origami nanostructures for customizable chemotherapeutic drug release. *Nucleic Acids Res*. 2021;49:3048–3062. https://doi.org/10.1093/nar/gkab097.
32. Sala L, Perecko T, Mestek O, Pinkas D, Homola T, Kočišek J. Cisplatin-cross-linked DNA origami nanostructures for drug delivery applications. *ACS Appl Nano Mater*. 2022;5:13267–13275. https://doi.org/10.1021/acsanm.2c02976.
33. Chen H, Zhang H, Pan J, Cha T-G, Li S, Andréasson J, et al. Dynamic and progressive control of DNA origami conformation by modulating DNA helicity with chemical adducts. *ACS Nano*. 2016;10:4989–4996. https://doi.org/10.1021/acsnano.6b01339.
34. Lee H, Lytton-Jean AKR, Chen Y, Love KT, Park AI, Karagiannis ED, et al. Molecularly self-assembled nucleic acid nanoparticles for targeted in vivo siRNA delivery. *Nat Nanotechnol*. 2012;7:389–393. https://doi.org/10.1038/nnano.2012.73.
35. Zhang G, Zhang Z, Yang J. DNA tetrahedron delivery enhances doxorubicin-induced apoptosis of HT-29 colon cancer cells. *Nanoscale Res Lett*. 2017;12:495. https://doi.org/10.1186/s11671-017-2272-9.
36. Sun P, Zhang N, Tang Y, Yang Y, Chu X, Zhao Y. SL2B aptamer and folic acid dual-targeting DNA nanostructures for synergic biological effect with chemotherapy to combat colorectal cancer. *Int J Nanomedicine*. 2017;12:2657–2672. https://doi.org/10.2147/IJN.S132929.
37.. Ehrlich P. *In Collected Papers of Paul Ehrlich*. London: Pergamon Press; 1956.
38. Céspedes MV, Unzueta U, Aviñó A, Gallardo A, Álamo P, Sala R, et al. Selective depletion of metastatic stem cells as therapy for human colorectal cancer. *EMBO Mol Med*. 2018;10. https://doi.org/10.15252/emmm.201708772.
39. Damha MJ, Giannaris PA, Zabarylo SV. An improved procedure for derivatization of controlled-pore glass beads for solid-phase oligonucleotide synthesis. *Nucleic Acids Res*. 1990;18:3813–3821. https://doi.org/10.1093/nar/18.13.3813.
40. Gupta KC, Kumar P, Bhatia D, Sharma AK. A rapid method for the functionalisation of polymer supports for solid phase oligonucleotide synthesis. *Nucleosides Nucleotides Nucleic Acids*. 1995;14:829–832. https://doi.org/10.1080/15257779508012482.
41. Gmeiner WH, Debinski W, Milligan C, Caudell D, Pardee TS. The applications of the novel polymeric fluoropyrimidine F10 in cancer treatment: current evidence. *Future Oncol*. 2016;12:2009–2020. https://doi.org/10.2217/fon-2016-0091.
42. Fàbrega C, Clua A, Eritja R, Aviñó A. Oligonucleotides carrying nucleoside antimetabolites as potential prodrugs. *Curr Med Chem*. 2021;28. https://doi.org/10.2174/0929867328666211129124039.
43. Meyerhardt JA, Mayer RJ. Systemic therapy for colorectal cancer. *N Engl J Med*. 2005;352:476–487. https://doi.org/10.1056/NEJMra040958.
44. Focaccetti C, Bruno A, Magnani E, Bartolini D, Principi E, Dallaglio K, et al. Effects of 5-fluorouracil on morphology, cell cycle, proliferation, apoptosis, autophagy and ROS production in endothelial cells and cardiomyocytes. *PloS One*. 2015;10,e0115686. https://doi.org/10.1371/journal.pone.0115686.
45. Singh Y, Murat P, Defrancq E. Recent developments in oligonucleotide conjugation. *Chem Soc Rev*. 2010;39:2054. https://doi.org/10.1039/b911431a.
46. Pommier Y, Leo E, Zhang H, Marchand C. DNA topoisomerases and their poisoning by anticancer and antibacterial drugs. *Chem Biol*. 2010;17:421–433. https://doi.org/10.1016/j.chembiol.2010.04.012.
47. Field JJ, Kanakkanthara A, Miller JH. Microtubule-targeting agents are clinically successful due to both mitotic and interphase impairment of microtubule function. *Bioorg Med Chem*. 2015;22:5050–5059. https://doi.org/10.1016/j.bmc.2014.02.035.
48. Aviñó A, Clua A, Bleda MJ, Eritja R, Fàbrega C. Evaluation of floxuridine oligonucleotide conjugates carrying potential enhancers of cellular uptake. *Int J Mol Sci*. 2021;22:5678. https://doi.org/10.3390/ijms22115678.

49. Walsh AS, Yin H, Erben CM, Wood MJA, Turberfield AJ. DNA cage delivery to mammalian cells. *ACS Nano*. 2011;5:5427–5432. https://doi.org/10.1021/nn2005574.
50. Liang L, Li J, Li Q, Huang Q, Shi J, Yan H, et al. Single-particle tracking and modulation of cell entry pathways of a tetrahedral DNA nanostructure in live cells. *Angew Chem Int Ed*. 2014;53:7745–7750. https://doi.org/10.1002/anie.201403236.
51. Rennick JJ, Johnston APR, Parton RG. Key principles and methods for studying the endocytosis of biological and nanoparticle therapeutics. *Nat Nanotechnol*. 2021;16:266–276. https://doi.org/10.1038/s41565-021-00858-8.
52. Fujimoto LM, Roth R, Heuser JE, Schmid SL. Actin assembly plays a variable, but not obligatory role in receptor-mediated endocytosis. *Traffic*. 2000;1:161–171. https://doi.org/10.1034/j.1600-0854.2000.010208.x.
53. Hao M, Mukherjee S, Sun Y, Maxfield FR. Effects of cholesterol depletion and increased lipid unsaturation on the properties of endocytic membranes. *J Biol Chem*. 2004;279:14171–14178. https://doi.org/10.1074/jbc.M309793200.
54. Ivanov AI. *Pharmacological inhibition of endocytic pathways: is it specific enough to be useful*?. 2008:15–33. https://doi.org/10.1007/978-1-59745-178-9_2.
55. Rajwar A, Shetty SR, Vaswani P, Morya V, Barai A, Sen S, et al. Geometry of a DNA nanostructure influences its endocytosis: cellular study on 2D, 3D, and *in vivo* systems. *ACS Nano*. 2022;16:10496–10508. https://doi.org/10.1021/acsnano.2c01382.
56. Bareford L, Swaan P. Endocytic mechanisms for targeted drug delivery☆. *Adv Drug Deliv Rev*. 2007;59:748–758. https://doi.org/10.1016/j.addr.2007.06.008.
57. Cheng Z, Li M, Dey R, Chen Y. Nanomaterials for cancer therapy: current progress and perspectives. *J Hematol Oncol*. 2021;14:85. https://doi.org/10.1186/s13045-021-01096-0.
58. Mathur D, Medintz IL. The growing development of DNA nanostructures for potential healthcare-related applications. *Adv Healthc Mater*. 2019;8. https://doi.org/10.1002/adhm.201801546.
59. Afonin KA, Dobrovolskaia MA, Church G, Bathe M. Opportunities, barriers, and a strategy for overcoming translational challenges to therapeutic nucleic acid nanotechnology. *ACS Nano*. 2020;14:9221–9227. https://doi.org/10.1021/acsnano.0c04753.